Available online at www.sciencedirect.com
SCIENCE DIRECT®
ELSEVIER
Applied Surface Science 219 (2003) 129–135
applied surface science
www.elsevier.com/locate/apsusc

Relative stability of missing-row reconstructed (1 1 0) surfaces of noble metals

A. Nduwimana*, X.G. Gong, X.Q. Wang

Department of Physics, Center for Theoretical Studies of Physical Systems, Clark Atlanta University, Atlanta, GA 3031, USA

Received 21 August 2002; accepted 17 December 2002

Abstract

The missing-row reconstruction has been observed experimentally on clean Au, Pt and Ir, while Cu and Ag are dormant cases in that the reconstruction can be provoked only by modest alkali coverage. The experimentally observed deconstruction and roughing transitions of Au(1 1 0) and Pt(1 1 0) are interesting realizations of two-dimensional Ising and *XY* models. The detailed understanding of the structures and energies of the missing-row configurations is also important for the constructions of many-atom model such as the embedded-atom potentials. We have carried out density-functional molecular-dynamics calculations for the missing-row reconstructed (1×2), (1×3), and ($1 \times \infty$) surfaces. The calculation results show that the delocalization of d-electrons and the accumulation of sp-electrons near the surface associated with the multilayer relaxation are important factors in stabilizing the experimentally observed (1×2) missing-row structure for Au and Pt. For Ir(1 1 0), a faceted (3 3 1) surface is shown to be the lowest energy configuration, in agreement with experimental observation. These results shed light on the relative stability of the missing-row configurations, and are useful for the construction of improved semi-empirical potentials, especially for the long range interaction.

Keywords: Missing-row reconstruction; Multilayer relaxation; Density-functional theory

1. Introduction

The ''missing-row'' reconstruction of noble metal (1 1 0) surfaces has been the subject of much theoretical and experimental attention [1–6]. The (1×2) missing-row reconstruction is found on clean Au, Pt, and Ir, while Cu and Ag are dormant cases in which the reconstruction can be provoked only by a modest alkali coverage [7]. Through the removal of every other row, the flat (1 1 0) surface is converted into a sequence of tiny (1 1 1) facets, which are favored by the lower (1 1 1) surface energy relative to that of (1 1 0). Experimental studies of the (1 1 0) configurations have revealed that the reconstruction is accompanied by heavy distortions (multilayer relaxations) [8,9]. Another characteristic feature of the missing-row reconstructed (1 1 0) surfaces is the discovery of roughening and deconstruction transitions [3,4,6]. For Au(1 1 0), the deconstruction of the (1×2) missing-row occurs at about 650 K, followed by a roughening transition at about 700 K. The critical exponents at the deconstruction transition temperature T_c are in concord with the two-dimensional (2D) Ising universality class [5]; while the roughening transition is of the Kosterlitz–Thouless (KT) type. For Pt(1 1 0), the two

* Corresponding author. Tel.: +1-404-880-8649.
E-mail address: xwang@ctsps.cau.edu (A. Nduwimana).

0169-4332/$ – see front matter © 2003 Published by Elsevier Science B.V.
doi:10.1016/S0169-4332(03)00598-1

processes proceed at the same temperature [10]. The intriguing interplay between the roughening and destruction led to the proposal of several phenomenological models [2,11–13].

Many implications of the complicated relaxation patterns of the missing-row surfaces on the roughening and deconstruction transitions are as yet unexplored. Recent experimental studies [3,4] have evidently demonstrated that the (1 × 1) configuration plays little role in the deconstruction and roughening transitions, contrary to the early models based on order–disorder transitions via lattice gas formation [6]. Instead, antiphase domains consisting of (1 × 3) steps are identified of crucial importance for Au(1 1 0). While the stability of the (1 × 2) missing-row configuration against the (1 × 1) unreconstructed structure has been understood theoretically [1], the relative stability between the (1 × 2) and (1 × 3) configurations has remained a paucity of theoretical study. Existing semi-empirical models are not yet capable of determining conclusively the energy orders and structural features [14,15].

In this paper, we report a systematic first-principles analysis on the relative stability of the (1 × 2) and (1 × 3) missing-row reconstructed configurations. Our calculation results show that the delocalization of d-electrons and the accumulation of sp-electrons near the surface associated with the multilayer relaxations, are important factors in stabilizing the experimentally observed (1 × 2) missing-row configurations for Au and Pt(1 1 0). For Ir(1 1 0), the missing-row configurations show weaker top-layer distortion. As a result, a faceted (3 3 1) structure is shown to be energetically favorable [16]. The present study reveals the correlation between the top-layer distortion and the relative stability of the missing-row configurations. Moreover, the analysis provides useful guidelines for the construction of the empirical models for the noble metals.

2. Calculation method

We have carried out first-principles calculations based on the density-functional theory for the unreconstructed and reconstructed (1 1 0) surfaces. The electronic density is expressed in terms of Kohn–Sham orbitals with an energy cutoff of 180, 200, and 210 eV, for Au, Pt, and Ir, respectively.

Table 1
Comparison of calculated properties of fcc bulk and atomic dimers for Au with the corresponding experimental data: the lattice constant a_0 (Å), bulk modulus B (GPa), and the cohesive energy E_c (eV) for the fcc bulk; the equilibrium bond-length d_0 (Å) and the binding energy E_0 for the atomic dimer

	a_0	B	E_c	d_0	E_0
GGA	4.15	136	3.20	2.55	2.63
LDA	4.07	174	4.39	2.46	3.16
Experimental	4.08[a]	173	3.81	2.47	2.29

[a] [20].

Only the valence electrons are treated explicitly and their interactions with ionic cores are described by the ultra-soft pseudo potentials with the scalar relativistic effect included. We have employed the local density (LDA) [17] and the generalized gradient approximations (GGA) [18] to the density-functional theory in the calculations. We performed tests for atomic dimer and bulk fcc phase of Au, Pt, and Ir [19]. Summarized in Table 1 are the results for the calculated bond-length and binding energy for the dimer, the lattice constant and the binding energy for the bulk structure of gold. The obtained results are in good agreement with

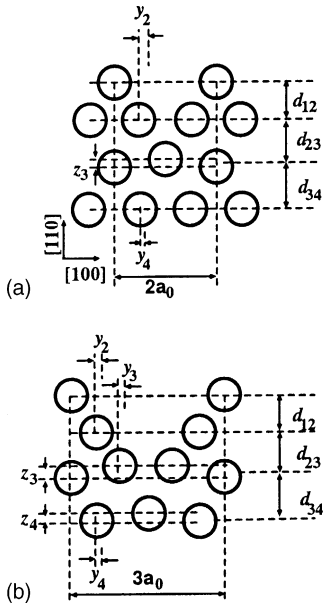

Fig. 1. Side views of (a) the (1 × 2) and (b) the (1 × 3) missing-row reconstructed geometries (schematic drawing). The characteristic quantities for multilayer relaxations are indicated.

experimental data [20]. For Pt and Ir, the calculated lattice constants are also in agreement with experimental results, with the lattice constants calculated within 1%, and the cohesive energy within 4% [21].

The (1 1 0) surfaces are modeled by slabs consisting of 13 atomic layers with six layers of vacuum. Shown in Fig. 1 are the schematic structures of (1 × 2) and (1 × 3). For the self-consistent calculations, the energy is converged to less than 5 meV/atom. The geometry optimization is carried out by atomic force calculations at $T = 0$ K, the forces acting on the atoms being converged to 0.01 eV/Å. It is worthwhile to mention that a large number of k-points are requested for the convergence. In our calculations, more than 14 k-points within the irreducible wedge of the Brillouin zone are found to be necessary.

3. Results

3.1. Multilayer relaxation

We start by presenting our results for the Au(1 1 0) configurations [19]. With use of LDA and GGA, both the (1 × 2) and (1 × 3) missing-row reconstructed structures undergo a large topmost-interlayer contraction, a slight row pairing in the second layer, and notable buckling in the third layer. The topmost-layer rows move straightly downward into the bulk region while the second layer atoms move slightly upward. The topmost-interlayer contraction (d_{12}) amounts to 7.3% for (1 × 1), 16.1% for (1 × 2), and 14.2% for (1 × 3). The calculated top-interlayer contraction of 16.1% for the (1 × 2) missing-row structure is in good agreement with available experimental data [8,9] and the first-principles results of Ho and Bohnen [1]. For the missing-row configurations, the atoms in the second layer have a small lateral displacement (indicated as y_2 in Fig. 1). The atoms in the third layer are buckled normal to the surface with a displacement of z_3 (see Fig. 1). The magnitude of the buckling for (1 × 2) is 4% of the interlayer spacing. For the (1 × 3) configuration, additional fourth layer contraction and buckling are observable. The detailed optimized structures are listed in Table 2.

As seen from Table 2, LDA calculation results yield similar trend in comparison with those of GGA. The only difference stands for the second interlayer spacing, d_{23}. The LDA predicts a contraction while the GGA predicts an expansion. Listed in Table 3 are the calculated top-layer distortions for Au, Pt, and Ir, respectively. It is worth noting that while Au and Pt have similar heavy top-layer distortions, Ir shows the largest top-layer distortion for (1 × 1) configuration. The different behavior for Ir suggests that the (1 × 2) reconstructed configuration is not stable against the (1 × n) configurations for $n \geq 3$.

As a matter of fact, the missing-row structure observed experimentally was argued to be a faceted (3 3 1) structure. Therefore, we have also calculated

Table 2
Multilayer relaxations (see Fig. 1 for the definitions) of missing-row Au(1 1 0) surfaces, measured in percentage of the interlayer distance without relaxation

	Structure	d_{12}	d_{23}	d_{34}	y_2	y_3	y_4	z_3	z_4
GGA	(1 × 1)	−7.3	+9	+0.0					
	(1 × 2)	−16.1	+5.0	+3.5	1.6		3.5	2.2	
	(1 × 3)	−14.2	+3.6	−3.1	2.3	1.5	0.5	1.8	1.6
LDA	(1 × 1)	−12.6	+5	−2.9					
	(1 × 2)	−17.5	−3.1	+0.0	1.1		1.0	3.4	
	(1 × 3)	−16.1	−1.9	−8.0	1.9	1.3	0.5	1.8	1.7
Experimental	(1 × 2)[a]	−18	4.0		1.7			7.0	
	(1 × 2)[b]	−20	2.0	2.0				8.0	
LDA	(1 × 2)[c]	−16	2	3	1.2			7	

[a] [8].
[b] [9].
[c] [1].

Table 3
The top-layer contraction (in %) for the (1 × 2), (1 × 3), and (1 × ∞) configurations of the missing-row reconstructed (1 1 0) surfaces

	Structure	Au	Pt	Ir
LDA	(l × 1)	−12.6	−8.0	−12.2
	(1 × 2)	−17.5	−17.0	−7.7
	(1 × 3)	−16.1	−16.5	−8.2
GGA	(l × 1)	−7.3	−12.0	−11.7
	(1 × 2)	−16.1	−17.0	−8.8
	(1 × 3)	−14.2	−16.3	−7.7

the structure and energies for Au, Pt, and Ir. For Au and Pt, this faceted structure is not energetically favorable. However, the structure is the most energetically favorable configuration for Ir. There exists very small top-layer distortion for the optimized Ir (3 3 1) faceted structure [21].

3.2. Surface energy

The surface energy, E_S, is calculated as $E_S = (1/2A)(E_{slab} - NE_{bulk})$, where A is the area of the surface, E_{slab} the energy of slab system and N is the total number of atoms in the system. We have carried out calculations of surface energies for missing-row configuration for Au, Pt and Ir. We summarize in Fig. 2 the calculated surface energies for various Au (1 1 0) configurations, with and without relaxation (geometry optimization). The (1 × ∞) configuration is equivalent to the close-packed (1 × 1) surface, with the surface area projected onto the (1 1 0) surface. $E_{1\times\infty} = 2E_{111} = 2E_{111}/\sqrt{3}$.

As seen from Fig. 2, the larger the n, the lower the surface energy of the unrelaxed (1 × n) configuration. Our calculations for the unrelaxed missing-row configurations of other 5d noble metals Pt and Ir have also confirmed this trend, which is in contrast to the 4d metals. This generic feature is attributed to the relativistic effect [7]. In contrast to Au and Pt, Ir(1 1 0) favors a faceted (3 3 1) configuration. This is confirmed by our calculation to be the structure of the lowest surface energy.

The relative surface-energy order for (1 × 2) and (1 × 3) is reversed after taking into account the multilayer relaxations. Our calculations have confirmed that the experimentally observed (1 × 2) missing-row

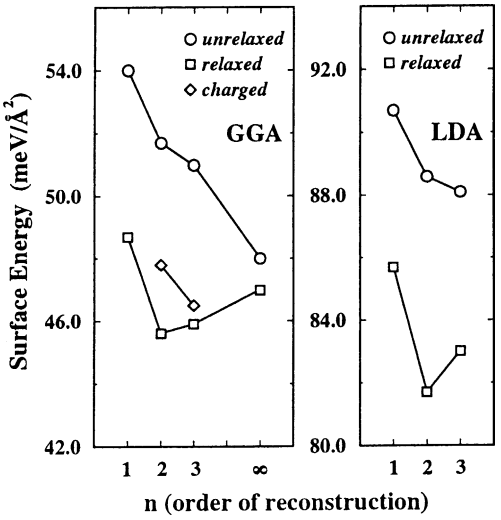

Fig. 2. Surface energy of relaxed (square), unrelaxed (circle), and 0.05e charge donated (diamond) (1 × n) Au(1 1 0) configurations, with GGA (left) and LDA (right). The lines are for guiding eyes. The (1 × 2) missing-row reconstructed surface has the lowest surface energy after the relaxation. The slight charge donation favors (1 × 3) missing-row configuration over the (1 × 2).

structure has the lowest surface energy for Au and Pt. In this respect, Ir stands for the only case among the noble metals that failed to achieve this reverse.

We summarized our results for calculated surface energies in Table 4. As is observable from Table 4, both calculation methods yield essentially the same trend for the missing-row reconstructed configurations. We show in Fig. 3 the calculated surface energy for Pt. Similar to the Au(1 1 0) case, for Pt the (1 × 2) and (1 × 3) configurations are very close in energy. The energy difference between the (1 × 2) and (1 × 3) configurations may be relevant to the study of the order–disorder and roughening transitions for Au and Pt(1 1 0) systems [19]. The detailed account of this aspect is beyond the scope of this paper and will be presented elsewhere. It is worthwhile to point out that the information on the relative energies of the missing-row configurations is useful for the construction of empirical models of these materials. As shown in Table 4, the calculated surface energies show systematic trends for systems going from Au, Pt, to Ir. It is also evident that there exists a strong correlation between the top-layer distortion and the energy difference between the relaxed and unrelaxed configurations.

Table 4
Surface energy (in eV/Å^2) for the missing-row reconstructed (1 1 0) surfaces using LDA and GGA, respectively

	Surface	Structure	Au	Pt	Ir
LDA	Unrelaxed	(1 × 1)	0.0915	0.16034	0.2375
		(1 × 2)	0.0885	0.1522	0.2327
		(1 × 3)	0.0881	0.1496	0.2289
		(1 × ∞)		0.1445	0.2324
		(3 3 1)		0.1587	0.2240
	Relaxed	(1 × 1)	0.0859	0.1526	0.2251
		(1 × 2)	0.0815	0.1418	0.2232
		(1 × 3)	0.0836	0.1414	0.2219
		(1 × ∞)		0.1437	0.2316
		(3 3 1)		0.1468	0.2143
GGA	Unrelaxed	(1 × 1)	0.0540	0.1080	0.1884
		(1 × 2)	0.0535	0.1014	0.1836
		(1 × 3)	0.0530	0.0997	0.1782
		(1 × ∞)	0.0481	0.0854	0.1841
	Relaxed	(1 × 1)	0.0495	0.1013	0.1786
		(1 × 2)	0.0456	0.0919	0.1764
		(1 × 3)	0.0458	0.0923	0.1731
		(l × ∞)	0.0481	0.8029	0.1841

The study of the lowest energy configuration for Ir deserves its own right. As is shown in Table 4, the faceted (3 3 1) configuration is slightly lower in energy as compared with (1 × ∞). The different trend of Ir as compared with Au and Pt is attributed to the much weaker d-electron localization effects (see discussions in the next sections).

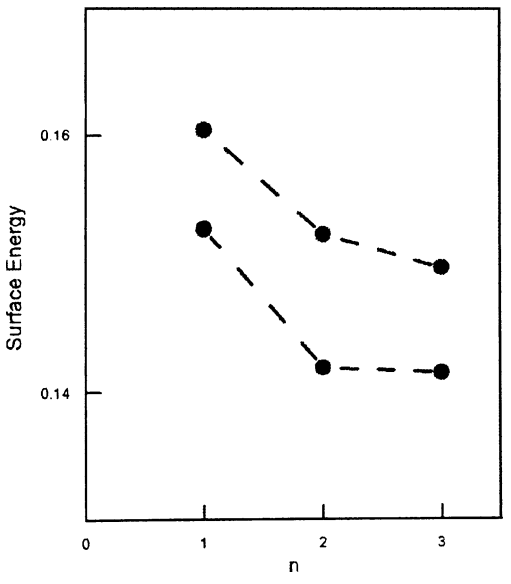

Fig. 3. Surface energy (in meV/Å^2) for the (1 × n) reconstructed (1 1 0) surface of Pt using GGA. The top line is for the unrelaxed configurations, and the lower one is for the relaxed structures.

3.3. Kinetic energy changes

To understand the effect of multilayer relaxation on the stability of missing-row reconstructed phases, we have conducted a thorough analysis of the resultant changes in kinetic energy and charge densities. For Au, the stability of the (1 × 2) missing-row structure over the (1 × 1) unreconstructed surface was investigated by Ho and Bohnen [1]. Based on a first-principles calculation, they discovered the reduction of the kinetic energies for both configurations. This reduction affects quantitatively, but not qualitatively, the relative stability of the two configurations. However, (1 × 3) has smaller kinetic energy than (1 × 2) owing to the more open trough structure, which also accounts for the lower surface energy than that of (1 × 2) for the

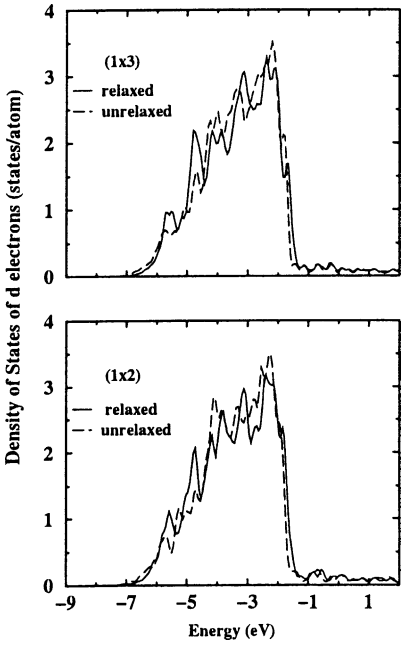

Fig. 4. Local density of d-electron states for surface atoms on the (1 × 3) (top) and (1 × 2) (bottom) missing-row reconstructed Au(1 1 0) configurations. The Fermi energy is shifted to zero. The increase of density states from unrelaxed structures (dashed lines) to relaxed ones (solid lines) in the bulk-like range (from −6.0 to −4.0 eV) along with the density shift to the high energy region indicate the delocalization of d-electrons on the surface.

Table 5
Angular momentum decomposed electronic valence charge N in the Wigner–Seitz radius for missing-row Au(1 1 0) surfaces

	$N^{u}_{(1\times2)}$	$N^{r}_{(1\times2)}$	$\Delta N_{(1\times2)}$	$N^{u}_{(1\times3)}$	$N^{r}_{(1\times3)}$	$\Delta N_{(1\times3)}$
s	0.609	0.615	0.006	0.612	0.616	0.004
p	0.251	0.268	0.017	0.251	0.264	0.013
d	8.946	8.941	−0.005	8.944	8.936	−0.008
Total	9.807	9.824	0.017	9.808	9.816	0.008

u and r stand for the unrelaxed and relaxed geometries, respectively. $\Delta N = N^{r} - N^{u}$ is the change due to the geometry optimization.

unrelaxed configuration. The multilayer relaxation yields a larger reduction of kinetic energy for (1×2) ($\Delta E_k = 145.9$ meV/Å^2) than for (1×3) ($\Delta E_k = 142.9$ meV/Å^2). In connection to this, there exists larger multilayer relaxation in (1×2) structure than (1×3). The calculation for Pt(1 1 0) shows the similar trends [21]. The difference in reduction of the kinetic energies associated with the multilayer relaxations plays a predominant role in addressing the relative stability of (1×2) and (1×3) missing-row configurations.

3.4. Delocalization of d-electrons

We show in Fig. 4 the local electronic density of d-electrons with and without relaxation for Au(1 1 0). d-Electrons tend to be localized in the surface layers, as the bandwidth of the surface density of states is narrowed and the center of d-states shifts upward in comparison with bulk. As is observable in Fig. 4, through relaxation, the d-electron density of states shift notably to the region between −6 and −4 eV, characterizing a delocalization of the d-electrons. The delocalization of the d-electrons through relaxation results in a large decrease of kinetic energy. A detailed analysis of the delocalization effects for Au, Pt, and Ir configurations shows that the effect is getting weaker going from Au, Pt, to Ir [21]. This is in conformity with the observed trend with regard to the top-layer distortions and the energy difference between the (1×2) and (1×3) configurations. It is interesting to note that Ir shows the weakest d-electron delocalization effect and the smallest top-layer distortion for the (1×2) and (1×3) configurations.

3.5. Increase of charge-density

On the other hand, the relaxation makes more sp-like electrons being piled up near the missing-row surface, suggesting a higher delocalized electronic density near the surface. The projected valence charge in the Wigner–Seitz sphere shows that the electrons, particularly p-like ones, spill out into the vacuum region due to the relaxations. As a result, an accumulation of charge is found for the top-layer atoms. Listed in Table 5 are the angular components of valence charge for the top-layer atoms for Au(1 1 0). As the larger sp density at surface corresponds to smaller kinetic energy [1], the larger increase of sp-electrons in (1×2) over (1×3) through relaxation leads to a larger reduction of the kinetic energy for (1×2).

The relative order of the surface energies of missing-row (1×2) and (1×3) structures is sensitive to the charges accumulated. To substantiate this point, we have calculated the surface energies[1] of (1×2) and (1×3) with a fraction charge (0.05e per (1×1) cell) donated onto the surface. As seen in Fig. 2, the donation of charges onto the surface leads to the preference of the (1×3) missing-row structure. This provides an interpretation of the experimental observation on charge-induced (1×3) structures [22,23]. Comparing the effect of charge-density increase, we observe again the trend of from strong to weak, for systems from Au, Pt, to Ir.

4. Conclusions

In summary, we have carried out an analysis of the relative stability between the (1×2) and (1×3) missing-row configurations for Au and Pt(1 1 O). Our calculation shows that the d-electron delocalization and sp-electron spilling-out associated with the

[1] The surface energy of the charged surface is not the absolute one. The energy difference between (1×2) and (1×3) structure is a true relevant quantity.

multilayer relaxation account for the stability of the experimentally observed (1 × 2) missing-row configurations. The calculated surface energies for Au, Pt, and Ir provide useful information on the electronic structure effects on the relative stability of the missing-row configurations. These results are useful for construction of empirical models capable of large-scale molecular dynamics simulations.

Acknowledgements

This work was supported by Air Force Office of Scientific Research Grant No. F49620-96-1-0211, US Army Grant No. DAAEO7-99-C-L065, and National Science Foundation Grant No. DMR-02-05328.

References

[1] K.M. Ho, K.P. Bohnen, Phys. Rev. Lett. 59 (1987) 1833; K.M. Ho, K.P. Bohnen, Europhys. Lett. 4 (1987) 345.
[2] Marcel den Nijs, Phys. Rev. Lett. 66 (1991) 907.
[3] M. Sturmat, R. Koch, K.H. Rieder, Phys. Rev. Lett. 77 (1996) 5071.
[4] C. Hbfher, J.W. Rabalais, Phys. Rev. B. 58 (1998) 9990.
[5] J.C. Campuzano, M.S. Foster, G. Jennings, R.F. Willis, W.N. Unerti, Phys. Rev. Lett. 54 (1985) 2684.
[6] J.C. Campuzano, A.M. Lahee, G. Jennings, Surf. Sci. 152–153 (1978) 265.
[7] C.L. Fu, K.M. Ho, Phys. Rev. Lett. 63 (1989) 1617.
[8] W. Moritz, D. Wolf, Surf. Sci. 163 (1985) L655.
[9] M. Copel, T. Gustafsson, Phys. Rev. Lett. 57 (1986) 723.
[10] I.K. Robinson, E. Vueg, K. Kern, Phys. Rev. Lett. 63 (1989) 2758.
[11] I. Vilfan, J. Villain, Phys. Rev. Lett. 65 (1990) 1830; J. Villain, I. Vilfan, Surf. Sci. 199 (1988) 165.
[12] G. Santoro, M. Vendruscolo, S. Prestipino, E. Tosatti, Phys. Rev. B 53 (1996) 13169.
[13] L. Balents, M. Kardar, Phys. Rev. B 46 (1992) 16031.
[14] M. Garofalo, E. Tosatti, F. Ercolessi, Surf. Sci. 188 (1987) 321.
[15] M. Daw, S.M. Foiles, Phys. Rev. Lett. 59 (1987) 2756.
[16] J.J. Scultz, M. Sturmat, R. Koch, Phys. Rev. B 62 (2000) 15402.
[17] D.M. Ceperley, B.J. Alder, Phys. Rev. Lett. 45 (1980) 566 as parameterized by J. Perdew, A. Zunger, Phys. Rev. B 23 (1981) 5048.
[18] J. Perdew, K. Burke, M. Ernzerhof, Phys. Rev. Lett. 77 (1996) 3865.
[19] X.G. Gong, D.Y. Sun, X.Q. Wang, Phys. Rev. B, submitted for publication.
[20] C. Kittle, Introduction to Solid Physics, Wiley, New York, 1986; J.W. Lynn, H.G. Smith, R.M. Nicklow, Phys. Rev. B 8 (1973) 3493.
[21] A. Nduwimana, M.S. Thesis, Clark Atlanta University, 2001.
[22] P. Haberle, P. Fenter, T. Gustafsson, Phys. Rev. B 39 (1989) 5810; J.V. Barth, R. Schuster, J. Wintterlin, R.J. Behm, G. Ertl, Phys. Rev. B 51 (1995) 4402.
[23] B.M. Ocko, G. Helgesen, B. Schardt, J. Wang, Phys. Rev. Lett. 69 (1992) 3350.